Magnetic ordering in the spin-chain compounds $Ca_3Co_{2-x}Fe_xO_6$ ($x=0.2$ and 0.4): A neutron diffraction study

A. Jain,[1] S. M. Yusuf,[1,*] J. Campo,[2] and L. Keller[3]
[1]*Solid State Physics Division, Bhabha Atomic Research Centre, Mumbai 400085, India*
[2]*Instituto de Ciencia de Materiales de Aragón, CSIC-Universidad de Zaragoza, C/Pedro Cerbuna 12, 50009 Zaragoza, Spain*
[3]*Laboratory for Neutron Scattering, ETH Zurich and Paul Scherrer Institut, CH-5232 Villigen PSI, Switzerland*
(Received 3 February 2009; published 27 May 2009)

We report the results of the neutron diffraction experiments on the spin-chain compounds $Ca_3Co_{2-x}Fe_xO_6$ ($x=0.2$ and 0.4) crystallizing in the rhombohedral structure (space group $R\bar{3}c$) in the temperature range of 1.5–100 K. Additional magnetic Bragg peaks in the low-temperature neutron powder diffraction patterns mainly indicate an antiferromagnetic ordering for these iron-substituted compounds. The observed magnetic reflections can be indexed in the nuclear lattice with a propagation vector $K=(0,0,1)$ which indicates that the centering translations have been lost in the magnetic structure. The Rietveld refinement of the neutron diffraction patterns for both the compounds confirms that the Γ_2 irreducible representation of the little group G^k classifies the magnetic structure which corresponds with ferromagnetic planes perpendicular to the b axis, where the magnetic moment is aligned along the c axis, coupled antiferromagnetically along the b direction. We demonstrate that two different magnetic structures, (i) amplitude modulated structure with a propagation vector $K=(0,0,1)$ and (ii) partially disordered antiferromagnet structure, are able to fit the same neutron diffraction pattern because the Fourier coefficients for each solution only differs in a global phase factor that cannot be determined by the experiment. The temperature-independent intensity of the (110) Bragg peak and the fact that the determined Fourier coefficients assure that the magnetic structure has net zero magnetic moment in the lattice confirm the absence of any phase transition to a ferrimagnetic state.

DOI: 10.1103/PhysRevB.79.184428 PACS number(s): 75.25.+z

I. INTRODUCTION

A_3MXO_6-type [A=Ca and Sr, and (M,X)=alkali or transition-metal ions] quasi-one-dimensional (1D) spin-chain compounds,[1–24] crystallizing in the K_4CdCl_6-type rhombohedral structure, have recently attracted much interest because of their peculiar magnetic properties. The crystal structure of these compounds consists of chains of alternating face sharing XO_6 octahedra (OCT) and MO_6 trigonal prism (TP) running along the crystallographic c axis. These chains, separated by A^{2+} ions, are arranged on a triangular lattice in the ab plane and each chain is surrounded by six chains. The ferromagnetic intrachain and antiferromagnetic interchain interactions combined with a triangular arrangement of the Ising spin chains can give rise to a geometrical frustration in these compounds. In the literature, there are a few examples where the 1D Ising spin chains are arranged on a triangular lattice. The most of the compounds belong to either the A_3MXO_6 family (considered in the present study) or the $A'BX_3$ (where A' is an alkali ion, B is a transition-metal ion, and X is a halide ion)[25–27] family. The compound $CsCoCl_3$ (Refs. 25 and 26) is one of the well-studied 1D Ising spin-chain compounds in the ABX_3 family. The results of most of theoretical models[25,27] for the $A'BX_3$ compounds predict the partially disordered antiferromagnet (PDA) structure [as shown in the Fig. 1(a)] at higher temperature and a ferrimagnetic (FI) structure [as shown Fig. 1(b)] at lower temperature (e.g., below 9 K for the compound $CsCoCl_3$). The crystal structure of the compound $CsCoCl_3$ consists of chains of Co^{2+} ions with effective spin $S=\frac{1}{2}$, arranged on a triangular lattice, running along the crystallographic c axis. Both the intrachain and interchain interactions in this compound are antiferromagnetic. However, the strength of the intrachain exchange interaction is much stronger than that of the interchain exchange interaction. This compound undergoes two successive magnetic phase transitions; one at 21 K and other at 9 K. In the temperature range between 9 and 21 K the PDA state and below 9 K a ferrimagnetic state have been found.

Among the A_3MXO_6-type spin-chain compounds, the most studied compounds are $Ca_3Co_2O_6$ (Ref. 2–21) and Ca_3CoRhO_6.[22–24] Unlike the compound $CsCoCl_3$, the intrachain interactions for the compounds $Ca_3Co_2O_6$ and Ca_3CoRhO_6 are reported to be ferromagnetic. Both the com-

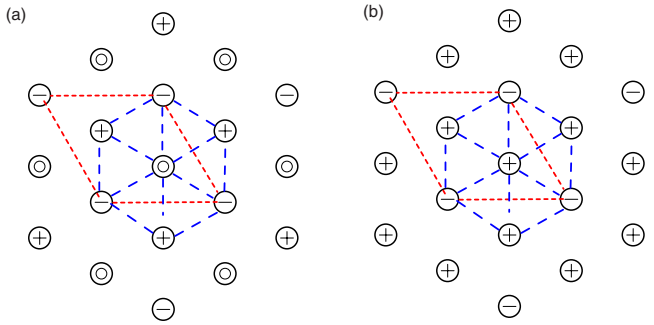

FIG. 1. (Color online) Schematic diagram of (a) PDA state and (b) ferrimagnetic (FI) state. The circles correspond to the Ising spin chains running along the crystallographic c axis. The plus and minus signs correspond to the direction of the magnetic moment along the crystallographic c axis; zero (0) represents the incoherent (the chain with net zero moment) spin chain. The red short-dashed lines represent the unit cell in the ab plane, and the blue long-dashed lines represent the triangular arrangement of spin chains.

pounds $Ca_3Co_2O_6$ and Ca_3CoRhO_6 crystallizes in the rhombohedral structure with space group $R\bar{3}c$. In the $Ca_3Co_2O_6$, Co^{3+} ions are located at 6*a* (TP) and 6*b* (OCT) crystallographic sites. In this compound, the spin chains, made up of alternating face sharing CoO_6 octahedra and CoO_6 trigonal prism, are separated by Ca^{2+} ions. It is reported that the different crystalline electric field at the OCT and TP sites leads to the different spin states of the Co^{3+} ions in this compound: low spin ($S=0$) and high spin ($S=2$) at the OCT and TP sites, respectively.[3] Due to the crystalline electric field, the Co^{3+} ions in this compound have very strong Ising-type anisotropy with moment (for the TP sites), preferentially aligned along the crystallographic *c* direction. The Co^{3+} ions in the adjacent spin chains are shifted by 1/6 or 1/3 along the *c* axis, perpendicular to the *ab* plane.[17] The compound $Ca_3Co_2O_6$ is reported to undergo two successive magnetic phase transitions at $T_{N1} \approx 25$ K and $T_{N2} \approx 10$ K.[19] In the temperature range between T_{N1} and T_{N2}, this compound would exhibit a PDA state [as shown in the Fig. 1(a)], a state where 2/3 ferromagnetic Ising spin-chain orders with antiferromagnetic interchain interaction while the remaining 1/3 are left incoherent (disordered with zero net magnetization).[19] There is sill an ambiguity regarding the nature of the magnetic state of this compound below T_{N2}, whether it is a frozen spin state (a state in which 1/3 incoherent spin chains freeze randomly) or a FI state [as shown Fig. 1(b)]. To the best of our knowledge, for the compound $Ca_3Co_2O_6$ there are only three reports in the literature on neutron diffraction studies; two on powder samples[3,14] and one on the single crystal.[13] The very first low-temperature neutron powder diffraction study for the compound $Ca_3Co_2O_6$ was carried out by Aasland *et al.*[3] Based on the analysis of neutron diffraction patterns, Aasland *et al.*[3] proposed a model for the magnetic structure; according to this model the magnetic structure consists of chains (ordered ferrimagnetically) of alternating magnetic moments of $(0.08 \pm 0.04)\mu_B$ and $(3.00 \pm 0.05)\mu_B$ for Co^{3+} at OCT and TP sites, respectively. The moments in a single chain lie along the *c* axis (coupled ferromagnetically). Kageyama *et al.*[14] also proposed the same model, and they ascribed a reduction in the intensity of the (100) peak below 13 K to a decrease in the ferrimagnetic domain size. The single-crystal neutron diffraction study for the compound $Ca_3Co_2O_6$ was carried out by Petrenko *et al.*[13] in an applied magnetic field $H \| c$, and they proposed the existence of the PDA state. However, based on the ratio of intensity of antiferromagnetic peaks for field-cooled and zero-field-cooled samples they concluded that the ground state of $Ca_3Co_2O_6$ was not a simple PDA state.

The effect of iron substitution on the structural and the magnetic properties of the compounds $Ca_3Co_{2-x}Fe_xO_6$ ($x=0$, 0.1, 0.2, and 0.4) has been investigated by some of us[17,28] using room-temperature neutron diffraction, x-ray powder diffraction, dc magnetization, and Mössbauer spectroscopy techniques. Kageyama *et al.*[15] and Arai *et al.*[16] investigated the magnetic properties of the compounds $Ca_3Co_{2-x}Fe_xO_6$ ($x \leq 0.1$) using the Mössbauer spectroscopy study. In the Mössbauer spectroscopy study, the well-resolved nuclear hyperfine structure corresponding to the exchange polarized Fe^{3+} electron spins ($m_z = \pm 5/2, \pm 3/2, \pm 1/2$) has been observed for $T \leq 20$ K. This observation is very remarkable in the present magnetically dense system. The observed hyperfine structure[15,16,28] has been ascribed to the different spin nature of the Fe^{3+} (Heisenberg) in comparison to the Co^{3+} (Ising). The magnetism of these Fe-substituted compounds is unique in the sense that spin chains are made up of different type of spins: Fe^{3+} (Heisenberg) and Co^{3+} (Ising). In our previous study,[17] based on the dc magnetization, the possibility of a spin state transition for the Co^{3+} moment at the octahedral site was shown in the Fe-substituted compounds. In general, the spin state transition in the cobalt oxides can be induced by pressure, temperature, or carrier concentration. There are various possible spin states for Co^{3+} ions in these cobalt oxides: low spin ($t_{2g}^6 e_g^0$, $S=0$), high spin ($t_{2g}^4 e_g^2$, $S=2$), and intermediate spin ($t_{2g}^5 e_g^1$, $S=1$) states. The transition from one spin state to another spin state occurs due to the competition between the crystal field energy and Hund's exchange energy leading to the distribution of the electrons in the t_{2g} and e_g orbital. To date, there is no report available in the literature on the neutron diffraction study of these iron-substituted compounds as a function of temperature. It is necessary to determine the spin structure of these compounds to understand the exotic magnetic properties of these spin-chain compounds. In this paper, we report the results of the neutron powder diffraction study as a function of temperature for the compounds $Ca_3Co_{2-x}Fe_xO_6$ ($x=0.2$ and 0.4). The aim of this study is to investigate the nature of the magnetic ground state of these iron-substituted compounds and to compare it with that of the parent compound $Ca_3Co_2O_6$. In this work we will demonstrate that the low-temperature neutron diffraction patterns for these iron-substituted compounds can be fitted with a PDA structure as well as with amplitude modulated structure. However, out of these two magnetic structures, which one is the ground state that will require detailed theoretical investigations?

II. EXPERIMENTAL

Polycrystalline samples of the compounds $Ca_3Co_{2-x}Fe_xO_6$ ($x=0.2$ and 0.4) were prepared by the conventional solid-state reaction method as described in an earlier paper.[17] Rietveld refinement of room-temperature x-ray powder diffraction pattern confirmed the single phase formation of these compounds in the rhombohedral structure (space group $R\bar{3}c$). The neutron diffraction experiments in the temperature range of 1.5–100 K were performed on the cold neutron powder diffractometer DMC at the Paul Scherrer Institute (PSI), Switzerland. For low-temperature measurements, a vanadium can containing the sample was placed in a helium "orange" cryostat. A constant wavelength of 2.46 Å was used, and the diffraction data were analyzed by the Rietveld method using the FULLPROF (Ref. 29) program. The representation theory analysis was performed using the BASIREPS software.[29]

III. RESULTS AND DISCUSSION

Figures 2 and 3 show, respectively, the Rietveld refined neutron powder diffraction patterns for the compounds

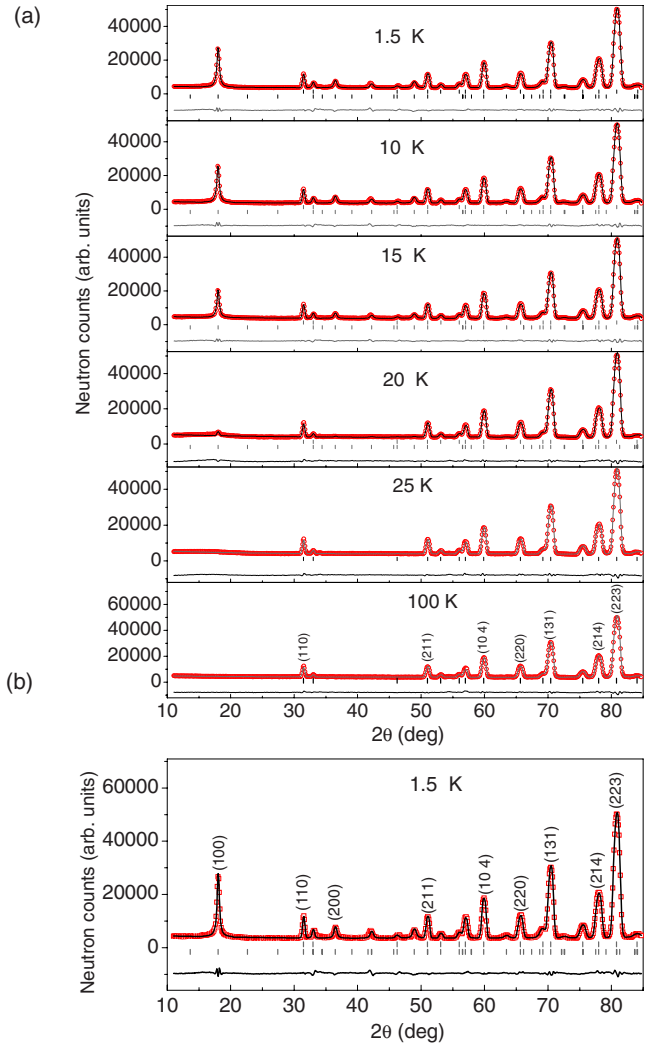

FIG. 2. (Color online) Observed (open circles) and calculated (solid lines) neutron diffraction patterns of $Ca_3Co_{1.8}Fe_{0.2}O_6$ using (a) amplitude modulated ($K=0,0,1$) (b) PDA structure. Solid line at the bottom of each panel shows the difference between the observed and the calculated patterns. The (hkl) values corresponding to stronger Bragg peaks are also listed. Vertical marks correspond to the position of all allowed Bragg reflections for the crystal (top row) and magnetic (bottom row) reflections. Neutron diffraction patterns at 100 and 25 K show only nuclear Bragg reflections.

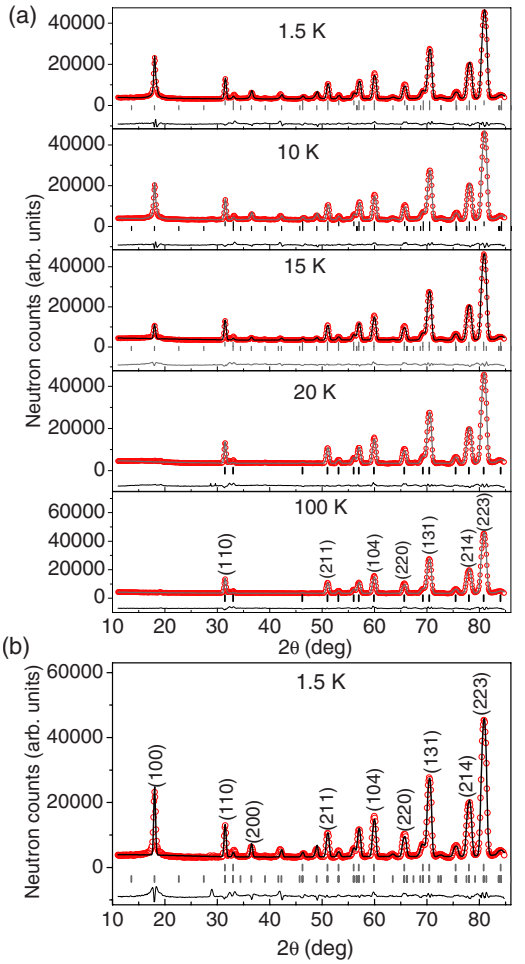

FIG. 3. (Color online) Observed (open circles) and calculated (solid lines) neutron diffraction patterns of $Ca_3Co_{1.6}Fe_{0.4}O_6$ using (a) amplitude modulated ($K=0,0,1$) (b) PDA structure. Solid line at the bottom of each panel shows the difference between the observed and the calculated patterns. The (hkl) values corresponding to stronger Bragg peaks are also listed. Vertical marks correspond to the position of all allowed Bragg reflections for the crystal (top row) and magnetic (bottom row) reflections. Neutron diffraction patterns at 100 and 20 K show only nuclear Bragg reflections.

$Ca_3Co_{2-x}Fe_xO_6$ with $x=0.2$ and 0.4. The lattice parameters and refined atomic positions at 100 K for all the atoms are listed in Table I. The refined values of the structural parameters are in good agreement with those previously reported from independent x-ray and neutron diffraction studies.[3,17] The Rietveld refinement of the neutron diffraction patterns confirmed that iron was located at the trigonal prism site ($6a$) which had already been confirmed by the Mössbauer spectroscopy in the previous study.[17] As shown in Figs. 2–4, the additional Bragg peaks start growing below 20 and 17 K for $x=0.2$ and $x=0.4$, respectively. These additional peaks, indexed with a propagation vector $K=(0,0,1)$ referred to the space group $R\bar{3}c$, can be ascribed to an antiferromagnetic ordering of the Co^{3+} and Fe^{3+} spins in these compounds. The magnetic structure has been analyzed using the standard irreducible representational theory as described by Bertaut.[30,31] For the propagation vector $\mathbf{K}=(0,0,1)$, the irreducible representations of the propagation vector group G^k are given in Table II. The magnetic reducible representation Γ for $6a$ and $6b$ sites can be decomposed as direct sum of irreducible representations as

$$\Gamma(6b|\mathrm{Co1}) = 1\Gamma_1^{(1)} + 1\Gamma_2^{(1)} + 2\Gamma_3^{(2)}$$

and

$$\Gamma(6a|\mathrm{Co2/Fe}) = 1\Gamma_1^{(1)} + 1\Gamma_2^{(1)} + 0\Gamma_3^{(2)}.$$

The representations Γ_1 and Γ_2 are one dimensional, while representation Γ_3 is two dimensional. According to the Bertaut method, in the first approximation, the vectors having the same representation of both sites may be coupled.[30,31] Therefore, we shall first consider the representations Γ_1 and Γ_2 to describe the magnetic structure for these compounds.

TABLE I. Results of the Rietveld refinement of neutron powder diffraction patterns at 100 K for $Ca_3Co_{2-x}Fe_xO_6$ (x=0.2 and 0.4) samples. Atomic positions for the space group $R\bar{3}c$: Ca at 18e $(x,0,\frac{1}{4})$, Co1 at 6b (0, 0, 0), Fe/Co2 at 6a (0, 0, 1/4), and O at 36f (x,y,z).

	Lattice constants (Å)					
x	a	c	Atom	x	y	z
0.2	9.0774(1)	10.3821(3)	Ca	0.3717(3)	0	$\frac{1}{4}$
			O	0.1768(3)	0.0226(3)	0.1147(2)
0.4			Ca	0.3715(3)	0	$\frac{1}{4}$
	9.0756(1)	10.3835(2)	O	0.1772(2)	0.0236(2)	0.1142(2)

The representation Γ_3 has not been used to describe the magnetic structure because it does not contribute at the 6a sites. The basis vectors of special positions 6a and 6b for the representations Γ_1 and Γ_2, calculated using the projection operator technique implemented in the BASIREPS,[29] are given in Table III. The observed neutron powder diffraction patterns for these compounds cannot be fitted with the magnetic structure corresponding to representation Γ_1. The magnetic structure corresponding to representation Γ_2, shown in Fig. 5(a), is suitable to describe the observed neutron powder diffraction patterns. The Rietveld refined neutron diffraction patterns for representation Γ_2 are shown in Figs. 2(a) and 3(a) for the x=0.2 and x=0.4 compounds, respectively. The magnetic moments for Co1 and Co2/Fe ions located at the 6b (0,0,0) and 6a $(0,0,\frac{1}{4})$ sites, respectively, are given by

$$\mathbf{m}_{L,\{j=6a,6b\}} = \sum_{\{-\mathbf{K},+\mathbf{K}\}} \frac{1}{2}\mathbf{S}_j^{\mathbf{K}} \exp\{-2\pi i\mathbf{K}\cdot\mathbf{R_L}\}$$
$$= \frac{1}{2}(\mathbf{S}_j^{\mathbf{K}} \exp\{-2\pi i\mathbf{K}\cdot\mathbf{R_L}\} + \mathbf{S}_j^{-\mathbf{K}} \exp\{2\pi i\mathbf{K}\cdot\mathbf{R_L}\})$$
$$= \mathbf{S}_j^{\mathbf{K}} \cos\{2\pi\mathbf{K}\cdot\mathbf{R_L}\}. \quad (1)$$

Here $\mathbf{S}_{6a}^{\mathbf{K}}$ and $\mathbf{S}_{6b}^{\mathbf{K}}$, the Fourier coefficients, are the maximum magnetic moments at the 6a and 6b sites, respectively,

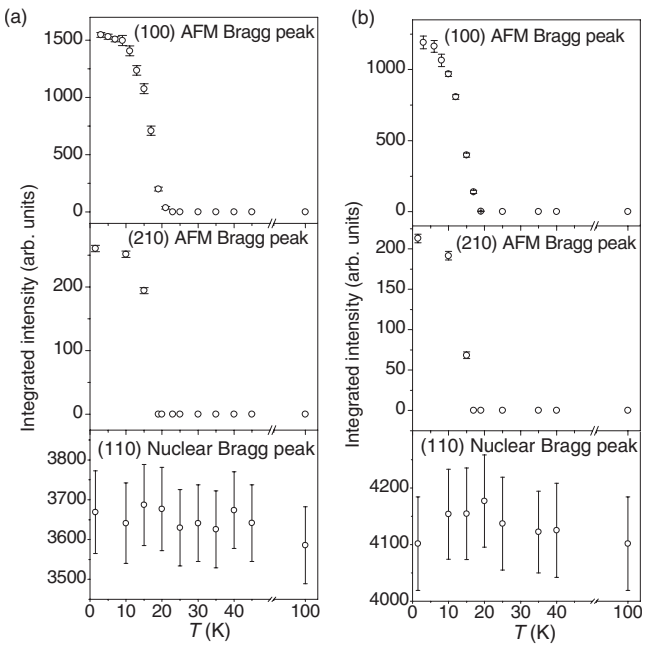

FIG. 4. Temperature dependence of the integrated intensity of the antiferromagnetic reflections (100) and (210) and nuclear Bragg peak (110) for (a) $Ca_3Co_{1.8}Fe_{0.2}O_6$ (b) $Ca_3Co_{1.6}Fe_{0.4}O_6$.

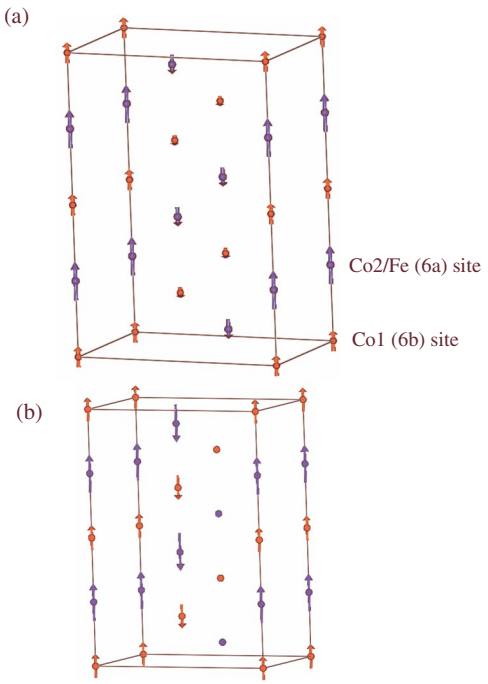

FIG. 5. (Color online) Magnetic structures corresponding to the representation (a) Γ_2 and (b) PDA model. Sites 6a and 6b are in blue and red, respectively. At 6a site there are two atoms Co and Fe with occupation factor $(1-x)$ and x, respectively. At 6b there is only one atom Co with an occupation factor of 1. Magnetic moments are scaled in order to show the small magnetic moment at 6a sites. (a) In representation Γ_2, the moments are aligned ferromagnetically along the c direction and are coupled antiferromagentically in the ab plane. (b) The PDA model, similar to Γ_2 but with 1/3 of the sites with zero averaged magnetic moment. Long arrow: 6a site, short arrow: 6b site.

TABLE II. Irreducible representation of the group of the propagation vector $\boldsymbol{G_k}$. $a=\exp(2\pi i/3)$; $b=\exp(4\pi i/3)$.

Symmetry element of G_k	1	$3^+_{0,0,z}$	$3^-_{0,0,z}$	$(x,-x,z)$	$(x,2x,z)$	$(2x,x,2z)$
Γ_1	1	1	1	1	1	1
Γ_2	1	1	1	−1	−1	−1
Γ_3	$\begin{pmatrix}1&0\\0&1\end{pmatrix}$	$\begin{pmatrix}a&0\\0&b\end{pmatrix}$	$\begin{pmatrix}b&0\\0&a\end{pmatrix}$	$\begin{pmatrix}0&1\\1&0\end{pmatrix}$	$\begin{pmatrix}0&b\\a&0\end{pmatrix}$	$\begin{pmatrix}0&a\\b&0\end{pmatrix}$

and R_L is the translation vector with respect to zeroth cell including the noninteger translations inside the magnetic unit cell $t1=(2/3,1/3,1/3)$ and $t2=(1/3,2/3,2/3)$. The values of $\mathbf{m}_{6a}$ and $\mathbf{m}_{6b}$ for the $x=0.2$ compound are $3.8(4)\mu_B$ and $0.04(2)\mu_B$, respectively. While for the $x=0.4$ compound, the values of $\mathbf{m}_{6a}$ and $\mathbf{m}_{6b}$ are $3.9(4)\mu_B$ per site ($6a$) and $0.02(1)\mu_B$ per site ($6b$), respectively. The magnetic moments at the translated related positions by $t1=(2/3\ 1/3\ 1/3)$ and $t2=(1/3\ 2/3\ 2/3)$ are amplitude modulated by a factor of $\cos(2\pi/3)=\cos(4\pi/3)=-0.5$. This kind of magnetic structure may arise due to the presence of the competing interactions in the presence of the large axial anisotropy. In the present compounds, ferromagnetic intrachain and antiferromagnetic interchain interactions combined with the triangular lattice arrangement of the Ising spin chains give rise to the competing interactions. As mentioned in Sec. I a stronger crystalline electric field at the OCT site ($6b$ site) can lead to the low spin state ($S=0$) of the Co^{3+} ions in this compound[3] and, therefore, gives an explanation of the nearly zero value of the observed moment at the $6b$ site. For the $6a$ site, the observed value of the magnetic moments is less than the theoretically calculated value using the expression $\mathbf{m}_{6a}=[(1-x)\mathbf{m}_{Co}+x\mathbf{m}_{Fe}]$. Here $\mathbf{m}_{Co}$ and $\mathbf{m}_{Fe}$ are the spin only values of the ordered moment for Co^{3+} and Fe^{3+}. The theoretically expected ordered moment values with quenched orbital moment for $\mathbf{m}_{6a}$ ($6a$ site) are $4.2\mu_B$ per site and $4.4\mu_B$ per site for $x=0.2$ and 0.4, respectively. The R factors for the refinement are: $R_{\text{Nuclear}}=1.35$ and $R_{\text{Magnetic}}=9.24$ for the $x=0.2$ and $R_{\text{Nuclear}}=2.96$, $R_{\text{Magnetic}}=14.7$ for the $x=0.4$ sample.

In a first inspection of the magnetic structure described above, it can be easily verified that the magnetic moments are not vanishing at any site and so no PDA model can be simulated using the propagation vector $\mathbf{K}=(0,0,1)$ and the space group $R\bar{3}c$. Therefore, in search of a possible PDA structure, we have tried to explain our experimental data using another model in which all the observed Bragg peaks have been indexed using the space group $P\bar{1}$ and a (0, 0, 0) propagation vector referred to the nuclear cell. The advantage of this model, in which we reduce the symmetry constraints, is that, for each site, the six initial positions before related by the translations $\mathbf{t}_1$ and $\mathbf{t}_2$ and the operator $(-y,-x,z+\frac{1}{2})$ are decoupled in three pairs of sites only related now by $(-y,-x,z+\frac{1}{2})$. Then the low-temperature neutron powder diffraction patterns for all these iron-substituted compounds have been refined considering the PDA model. A schema of the PDA magnetic structure has been shown in Fig. 5(b). In the PDA structure, 2/3 ferromagnetic Ising spin-chain orders with antiferromagnetic interchain interaction while the remaining 1/3 is left incoherent (disordered with zero net moment).

TABLE III. Basis vectors of positions $6a$ and $6b$ for representations Γ_1 and Γ_2.

IR	Basis vectors $\psi^{k,j}_{a,m}$ for $6b$ site		Basis vectors $\psi^{k,j}_{a,m}$ for $6a$ site	
	(0,0,0)	(0,0,1/2)	(0,0,1/4)	(0,0,3/4)
Γ_1	(0 0 1)	(0 0 −1)	(0 0 1)	(0 0 −1)
Γ_2	(0 0 1)	(0 0 1)	(0 0 1)	(0 0 1)

The Rietveld refined neutron diffraction patterns at 1.5 K using the PDA structure for the $x=0.2$ and the $x=0.4$ samples are shown in Figs. 2(b) and 3(b), respectively. The results of the magnetic Rietveld refinement are given in Table IV. The moments for both the sites $6a$ and $6b$ lie along the c axis. Both $6a$ and $6b$ sites for this compound are fully occupied. The refined values of the site averaged order moment for the

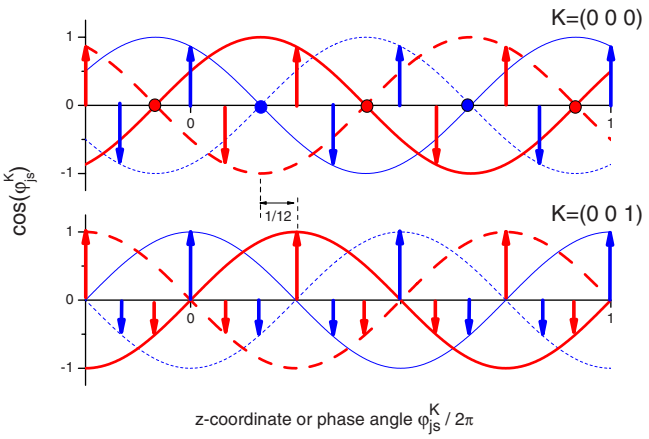

FIG. 6. (Color online). Magnetic moment modulation as function of the z coordinate (or equivalently, as can be observed in Table IV, the $\varphi^K_{js}/2\pi$ phase angle) for $6a$ (red; thick line) and $6b$ (blue; thin line) sites. From the figure it is easily observed that an $\pi/6$ global phase shift, the same for all the sites, allows to pass from model with $K=(0,0,0)$ on the top to model with $K=(0,0,1)$ at the bottom. For that reason the two models give the same magnetic pattern in powder neutron diffraction experiments. Lines are guides to the eyes to better show the modulation of each site. Also it is observed that the averaged magnetic moment along a unit cell is zero following, for each site ($6a$ and $6b$), the sequence $\ldots\sqrt{3}/2,0,-\sqrt{3}/2,\sqrt{3}/2,0,-\sqrt{3}/2\ldots$ for the model $K=(0\ 0\ 0)$ and $\ldots,1,-\frac{1}{2},-\frac{1}{2},1,-\frac{1}{2},-\frac{1}{2}\ldots$ for the model with $K=(0,0,1)$.

TABLE IV. Fourier coefficients (vector and phase) and results of the magnetic Rietveld refinement of neutron powder diffraction patterns at 1.5 K for $Ca_3Co_{2-x}Fe_xO_6$ using (a) amplitude modulated ($K=0,0,1$) (model 1) and (b) PDA structure (model 2). At 6*a* site there are two atoms Co and Fe with occupation factor $(1-x)$ and x, respectively. At 6*b* there is only one atom Co with an occupation factor of 1. The moments are aligned in the c direction for both sites; as a result m_x and m_y are zero for both sites. [Constant is $c=1$ and $c=2\sqrt{3}$ for the amplitude modulated ($K=0,0,1$) and the PDA structure, respectively.]

		$S_{js}^K=m_z(00c)\exp(-i2\pi\varphi_{js}^K)$					
		$\varphi_{js}^K/2\pi$		m_z/μ_B			
		$\varphi_{js}^K=\phi_{js}^K+\psi_j^K$		$X=0.2$		$X=0.4$	
		Model 1	Model 2	Model 1	Model 2	Model 1	Model 2
6*a*	$(0,0,\frac{1}{4})$ $(0,0,\frac{3}{4})$	0	1/12	3.8(2)	3.8(2)	3.9(4)	3.7(6)
	(2/3,1/3,7/12) (2/3,1/3,1/12)	1/3	1/4	−1.9	0.0	−1.95	0.0
	(1/3,2/3,11/12) (1/3,2/3,5/12)	2/3	7/12		−3.8(2)		−3.7(6)
6*b*	(0,0,0) $(0,0,\frac{1}{2})$	0	1/12	0.04(2)	0.04(2)	0.02(1)	0.02(1)
	(2/3,1/3,1/3) (2/3,1/3,5/6)	1/3	1/4	−0.02	0.0	−0.01	0.0
	(1/3,2/3,2/3) (1/3,2/3,1/6)	2/3	7/12		−0.04(2)		−0.02(1)
R mag				9.24	9.98	14.7	15.2

6*a* site (four out of six) at 1.5 K are 3.8(2) and 3.7(6)μ_B per site for $x=0.2$ and 0.4, respectively. The refined values of the ordered moment for the 6*b* site are very small for both the compounds (Table IV). The *R* factors are: $R_{\text{Nuclear}}=1.73$ and $R_{\text{Magnetic}}=9.98$ for $Ca_3Co_{1.8}Fe_{0.2}O_6$ and $R_{\text{Nuclear}}=3.06$ and $R_{\text{Magnetic}}=15.2$ for $Ca_3Co_{1.6}Fe_{0.4}O_6$. In this model also the observed ordered moments for 6*a* site at 1.5 K are less than the calculated spin only values.

Hence, we realize that two different magnetic structures, one in the $R\bar{3}c$ and the other in $P\bar{1}$, are able to fit our experimental intensities. In fact they are not so different because their Fourier coefficients are only differing in a global phase factor of $\psi_j^K=\pi/6$, which cannot be fixed by symmetry and it is the same for the two different sites. That is, $\mathbf{S}_{js}^{\mathbf{K}=(001)}=\mathbf{S}_{js}^{\mathbf{K}=(000)}\exp\{-i\pi/6\}$ where "*js*" is 6*a* or 6*b*. Another important common point in the two structures is that the total magnetization, independent of the model, is zero in the unit cell, which excludes a possible ferrimagnetic configuration. In Fig. 6, the effect of this global phase shift is represented.

As described in the literature,[13,14] both the PDA and ferrimagnetic structures have been observed for the parent compound $Ca_3Co_2O_6$. The PDA state for the parent compound $Ca_3Co_2O_6$ has also been confirmed by muon spin relaxation study.[12,18] The important point here is that if the iron-substituted compounds adopt the ferrimagnetic structure then some of the fundamental Bragg peaks, especially the fundamental (110) Bragg peak, should have a magnetic contribution below the magnetic ordering temperature. A simple calculation shows that magnetic contribution in the intensity of (110) Bragg peak is zero in the PDA state, while in the ferrimagnetic state the magnetic contribution is finite. Figure 4 shows the temperature dependence of the integrated intensity of peak (110) for the $x=0.2$ and 0.4 samples. It is evident from the figures that there is no change in the integrated intensity of the (110) peak down to 1.5 K for both the compounds. This clearly rules out the possibility of the ferromagnetic or ferromagnetic state. The observed reduction in the value of the ordered moment for the 6*a* site in both the models may be due to spin-orbit coupling and covalence effects.[32–36] The small moment on the 6*b* site may come from the spin state transition of some of the Co^{3+} ions at octahedral site (6*b* site) from low spin ($S=0$) to high spin ($S=2$)/intermediate spin ($S=1$) state.

Now we discuss an important point which goes beyond the models used here. Figure 4 shows the temperature dependence of the integrated intensity of the prominent antiferromagnetic Bragg peak (100) for the present iron-substituted compounds. The (100) peak appears below 20 and 17 K for $x=0.2$ and $x=0.4$ samples. Here it may be noted from the literature[3,13,14] that for the parent compound $Ca_3Co_2O_6$, the intensity of the (100) peak first increases with decreasing

temperature; however, below 18 K the intensity of the (100) peak decreases with decreasing temperature. This has been ascribed to a transition from the PDA to the ferrimagnetic structure for $Ca_3Co_2O_6$. In the present study, the observed intensity variation (Fig. 4), combined with no change in the intensity of the (110) fundamental peak, indicates that there is no phase transition to a ferrimagnetic or ferromagnetic state (in the zero applied magnetic field) for the iron-substituted compounds.

The Rietveld refinement of the neutron diffraction patterns suggests that the PDA structure, as well as the amplitude modulated structure $[K=(0,0,1)]$, is suitable for the magnetic structure of the Fe-substituted compounds (their magnetic R factors are very close). A theoretical study is required to find out the most stable ground-state configuration (out of these two possible magnetic structures) for these compounds. If the ground state of these iron-substituted compounds is a PDA state [Fig. 1(a)], then the overall degeneracy of the ground state will be very large because the center chain in Fig. 1(a) can be chosen in a large numbers of ways. The large degeneracy of the ground state may give rise to residual entropy in the specific-heat measurement. The polarized neutron diffraction study using a single crystal may be useful as it can measure the phase factor and hence can possibly determine the ground state of these compounds.

IV. CONCLUSION

We have investigated the magnetic structure of the quasi-one-dimensional spin-chain compounds $Ca_3Co_{2-x}Fe_xO_6$ ($x=0.2$ and 0.4) by neutron powder diffraction experiments in the temperature range of 1.5–100 K. Additional magnetic diffraction peaks in the low-temperature neutron powder diffraction patterns indicate the presence of the antiferromagnetic structure for these iron-substituted compounds. Two models are proposed to explain the observed magnetic structure. The observed neutron powder diffraction patterns for both compounds are consistent with the amplitude modulated structure $[K=(0,0,1)]$ [Fig. 5(a)] as well as the PDA structure $[K=(0,0,0)$ (Fig. 5(b)]. No phase transition from the PDA state to a ferrimagnetic state for these iron-substituted compounds has been found. We demonstrate that the same experimental neutron diffraction data can represent two very different magnetic structures differing only in a global phase. The common point is that magnetization in the unit cell is zero for both magnetic structures. The important point is that neutron powder diffraction experiments are unable to distinguish between the proposed model structures because of the fact that a global phase factor cannot be determined by the experiment. A unique determination of the ground state will require detailed investigations. The magnetic moment reduction at the 6*a* site may be due to spin-orbit coupling and covalence effects.

*Corresponding author. FAX: +91 22 25505151; smyusuf@barc.gov.in

[1] K. E. Stitzer, J. Darriet, and H.-C. zur Loye, Curr. Opin. Solid State Mater. Sci. **5**, 535 (2001).
[2] S. Majumdar, V. Hardy, M. R. Lees, D. McK. Paul, H. Rousseliere, and D. Grebille, Phys. Rev. B **69**, 024405 (2004).
[3] S. Aasland, H. Fjellvåg, and B. Hauback, Solid State Commun. **101**, 187 (1997).
[4] H. Kageyama, K. Yoshimura, K. Kosuge, M. Azuma, M. Takano, H. Mitamura, and T. Goto, J. Phys. Soc. Jpn. **66**, 3996 (1997).
[5] V. Hardy, S. Lambert, M. R. Lees, and D. McK. Paul, Phys. Rev. B **68**, 014424 (2003).
[6] B. Martínez, V. Laukhin, M. Hernando, J. Fontcuberta, M. Parras, and J. M. González-Calbet, Phys. Rev. B **64**, 012417 (2001).
[7] B. Raquet, M. N. Baibich, J. M. Broto, H. Rakoto, S. Lambert, and A. Maignan, Phys. Rev. B **65**, 104442 (2002).
[8] V. Hardy, M. R. Lees, O. A. Petrenko, D. McK. Paul, D. Flahaut, S. Hebert, and A. Maignan, Phys. Rev. B **70**, 064424 (2004).
[9] E. V. Sampathkumaran, N. Fujiwara, S. Rayaprol, P. K. Madhu, and Y. Uwatoko, Phys. Rev. B **70**, 014437 (2004).
[10] R. Frésard, C. Laschinger, T. Kopp, and V. Eyert, Phys. Rev. B **69**, 140405(R) (2004).
[11] V. Hardy, D. Flahaut, M. R. Lees, and O. A. Petrenko, Phys. Rev. B **70**, 214439 (2004).
[12] J. Sugiyama, H. Nozaki, J. H. Brewer, E. J. Ansaldo, T. Takami, H. Ikuta, and U. Mizutani, Phys. Rev. B **72**, 064418 (2005).
[13] O. A. Petrenko, J. Wooldridge, M. R. Lees, P. Manuel, and V. Hardy, Eur. Phys. J. B **47**, 79 (2005).
[14] H. Kageyama, K. Yoshimura, K. Kosuge, X. Xu, and S. Kawano, J. Phys. Soc. Jpn. **67**, 357 (1998).
[15] H. Kageyama, S. Kawasaki, K. Mibu, M. Takano, K. Yoshimura, and K. Kosuge, Phys. Rev. Lett. **79**, 3258 (1997).
[16] J. Arai, H. Shinmen, S. Takeshita, and T. Goko, J. Magn. Magn. Mater. **272-276**, 809 (2004).
[17] A. Jain, S. Singh, and S. M. Yusuf, Phys. Rev. B **74**, 174419 (2006).
[18] S. Takeshita, J. Arai, T. Goko, K. Nishiyama, and K. Nagamine, J. Phys. Soc. Jpn. **75**, 034712 (2006).
[19] H. Kageyama, K. Yoshimura, K. Kosuge, H. Mitamura, and T. Goto, J. Phys. Soc. Jpn. **66**, 1607 (1997).
[20] A. Maignan, V. Hardy, S. Hébert, M. Drillon, M. R. Lees, O. Petrenko, D. McK. Paul, and D. Khomskii, J. Mater. Chem. **14**, 1231 (2004).
[21] S. Agrestini, C. Mazzoli, A. Bombardi, and M. R. Lees, Phys. Rev. B **77**, 140403(R) (2008).
[22] M. Loewenhaupt, W. Schäfer, A. Niazi, and E. V. Sampathkumaran, Europhys. Lett. **63**, 374 (2003).
[23] S. Niitaka, K. Yoshimura, K. Kosuge, M. Nishi, and K. Kakurai, Phys. Rev. Lett. **87**, 177202 (2001).
[24] S. Niitaka, H. Kageyama, K. Yoshimura, K. Kosuge, S. Kawano, N. Aso, A. Mitsuda, H. Mitamura, and T. Goto, J. Phys. Soc. Jpn. **70**, 1222 (2001).
[25] M. Mekata, J. Phys. Soc. Jpn. **42**, 76 (1977).
[26] M. Mekata and K. Adachi, J. Phys. Soc. Jpn. **44**, 806 (1978).
[27] M. L. Plumer and A. Caillé, J. Appl. Phys. **70**, 5961 (1991).
[28] I. Nowik, A. Jain, S. M. Yusuf, and J. V. Yakhmi, Phys. Rev. B **77**, 054403 (2008).
[29] J. Rodriguez-Carvajal, Physica B **192**, 55 (1993).
[30] E. F. Bertaut, in *Magnetism*, edited by G. T. Rado and H. Suhl

(Academic, New York, 1963), Vol. 3.
[31] E. F. Bertaut, Acta Crystallogr., Sect. A: Cryst. Phys., Diffr., Theor. Gen. Crystallogr. **24**, 217 (1968).
[32] M. Cwik, T. Lorenz, J. Baier, R. Muller, G. Andre, F. Bouree, F. Lichtenberg, A. Freimuth, R. Schmitz, E. Muller-Hartmann, and M. Braden, Phys. Rev. B **68**, 060401(R) (2003).
[33] H. A. Alperin, Phys. Rev. Lett. **6**, 55 (1961).
[34] J. Campo, J. Luzón, F. Palacio, A. Millán, and G. J. McIntyre, Polyhedron **22**, 2297 (2003).
[35] J. Campo, J. Luzón, F. Palacio, G. J. McIntyre, and Eric Ressouche, Physica B **335**, 15 (2003).
[36] J. Luzón, J. Campo, F. Palacio, G. J. Mc Intyre, and A. Millán, Phys. Rev. B **78**, 054414 (2008).